Linear Pentapods with a Simple Singularity Variety – Part II: Computation of Singularity-Free Balls

Arvin Rasoulzadeh and Georg Nawratil

Center for Geometry and Computational Design, Vienna University of Technology, Austria,
{rasoulzadeh,nawratil}@geometrie.tuwien.ac.at

Abstract. The configuration space of a linear pentapod can be defined as the set of all points $(u,v,w,p_x,p_y,p_z) \in \mathbb{R}^6$ located on the singular quadric $\Gamma : u^2 + v^2 + w^2 = 1$, where (u,v,w) determines the orientation of the linear platform and (p_x,p_y,p_z) its position. In such terminology, the set of all singular robot configurations is obtained by intersecting Γ with a cubic hypersurface Σ in $\mathbb{R}^6$, which is only quadratic in the orientation variables and position variables, respectively. We study the computational aspects of the determination of singularity-free balls under the design restrictions that Σ is either (1) linear in position variables or (2) linear in orientation variables. It turns out that for these pentapod designs the computation of singularity-free balls in the configuration space simplifies considerably. One can even obtain a closed form solution, which is paving the way for a real-time singularity-free path planning/optimization in the configuration space.

Keywords: Linear pentapods, Distance computation, Singularity-free balls

1 Introduction

A *linear pentapod* is defined as a five degree-of-freedom (DOF) parallel manipulator consisting of a linear motion platform ℓ, which is connected via five spherical-prismatic-spherical (SPS) legs with the base, where the P-joints are active and the S-joints are passive. The pose of ℓ is uniquely determined by a position vector $\mathbf{p} \in \mathbb{R}^3$ and an orientation given by a unit-vector $\mathbf{i} \in \mathbb{R}^3$. The coordinate vector $\mathbf{m}_j$ of the platform anchor point m_j of the j-th leg is defined by the equation $\mathbf{m}_j = \mathbf{p} + r_j\mathbf{i}$ with $r_j \in \mathbb{R}$ and the base anchor points M_j of the j-th leg has coordinates $\mathbf{M}_j = (x_j,y_j,z_j)^T$ for $j = 1,\dots,5$.

It turns out that this kind of manipulator is an interesting alternative to serial robots handling axis-symmetric tools. Some fundamental industrial tasks such as 5-axis milling, laser engraving and water jet cutting are counted as its applications in industry [1], [2].

Special configurations referred to as *kinematic singularities* have always been central in mechanism theory and robotics. In such singularities, the *kinetostatic* properties of a mechanism undergo sudden and dramatic changes. This motivates the enormous practical value of a careful study and thorough understanding of the phenomenon for the design, control and application of robot manipulators.

In a singular configuration of a linear pentapod the platform is *infinitesimal movable* while all prismatic joints are locked; i.e. the manipulator gains an uncontrollable instantaneous DOF. Such a *shaky* configuration can also be characterized as a multiple solution of the direct kinematics problem. In this context it should be mentioned that

the forward kinematics of a linear pentapod was solved for the first time in [3] under the assumption of a planar base, and in [4] for the general case. If the direct kinematics problem has a continuous solution, then the linear pentapod has a so-called self-motions (for details see [4] and [5], respectively). The importance of the singularity study of a mechanism becomes evident in view of this most dangerous singular phenomenon as the uncontrollable moving platform is a hazard to man and machine.

A further well-studied aspect in the singularity analysis of linear pentapods are designs, which are singular in any configuration. A complete list of so-called architecture singular designs is given in [4, Section 1.3].

1.1 Preparatory work and outline

The configuration space of a linear pentapod can be defined as the set of all points $(u,v,w,p_x,p_y,p_z) \in \mathbb{R}^6$ located on the singular quadric $\Gamma : u^2+v^2+w^2 = 1$, where (u,v,w) determines the orientation of the linear platform and (p_x,p_y,p_z) its position. In such terminology, the set of all singular robot configurations is obtained by intersecting Γ with a cubic hypersurface Σ in $\mathbb{R}^6$, which is only quadratic in the orientation variables and position variables, respectively[1]. In [7] we determined all designs of linear pentapods with the property that Σ is either (1) linear in position variables or (2) linear in orientation variables. The obtained results can be summarized as follows:

Theorem 1. *A non-architecturally singular linear pentapod has a singularity polynomial linear in position variables, iff there is a singular affine mapping κ from the planar base to the platform line ℓ with $M_i \mapsto m_i$ for $i = 1,\dots,5$.*

Theorem 2. *A non-architecturally singular linear pentapod has a singularity polynomial linear in orientation variables in the following cases possessing a planar base:*

1. *M_2, M_3, M_4, M_5 are collinear,*
2. *$m_1 = m_i$ and M_j, M_k, M_l are collinear with pairwise distinct $i,j,k,l \in \{2,3,4,5\}$,*
3. *$m_1 = m_i = m_j$ with pairwise distinct $i,j \in \{2,3,4,5\}$.*

Clearly, due to the degree reduction it becomes easier to obtain closed form information about singular poses. But the main motivation for our research is the computational simplification of singularity-free balls, for which the state of art is as follows:

In [6] it is proven that for a generic linear pentapod, the computation of the maximal singularity-free ball in the position/orientation workspace (with respect to the ordinary Euclidean/Riemannian distance) leads over to the solution of a polynomial of degree 6 and 8, respectively. The corresponding closest singular configurations in the position/orientation workspace are illustrated in Fig. 1-left.

In contrast the determination of the closest singular pose (cf. Fig. 1-right) within the complete configurations space (with respect to an object-oriented metric) leads across the solution of a polynomial of degree 80, which is far away of a desired closed form solution, which offers interesting new concepts and strategies concerning path optimization [8] and singularity avoidance. Our first idea to cope with this problem was

[1] A rational parametrization of the singularity loci $\Gamma \cap \Sigma$ was given by the authors in [6].

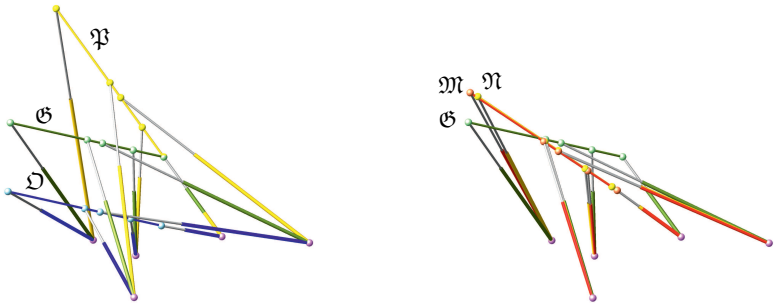

Fig. 1. Given is the pose $\mathfrak{G}$ (black) of the linear pentapod. Left: The closest singular configurations in the position/orientation workspace are given by the pose $\mathfrak{P}$ (yellow) and $\mathfrak{O}$ (blue), respectively. Right: $\mathfrak{M}$ (red) is the closest singular pose under Euclidean motions of ℓ and $\mathfrak{N}$ (yellow) is the closest singularity under equiform motions of ℓ.

to relax the motion group from the Euclidean one to the group of equiform motions (similarity transformations), which is equivalent to omitting the normalizing condition Γ. Doing so, the degree drops to 28, which was demonstrated in the extended version of [6] and is displayed in Fig. 1-right. As the obtained distance of the relaxed problem is less or equal to the distance of the original problem, it can be used as the radius of a guaranteed singularity-free ball.

Before plunging into the computations of the *singularity-free balls* for linear pentapods possessing a singularity polynomial linear in position/orientation variables (cf. Section 2 and Section 3, respectively) a further definition seems to be necessary:

Consider the *Lagrange equation* $L := f + \lambda_1 \Phi_1 + ... + \lambda_n \Phi_n$, where f is a smooth *distance function* on a manifold M which equals $\mathbb{R}^6$, $\mathbb{R}^3$ or S^2. Moreover a certain subset N of M is given as the zero-set of the polynomials $\Phi_1, \ldots, \Phi_n$ and their corresponding *Lagrange multipliers* are denoted by $\lambda_1, \ldots, \lambda_n$. Then the solutions of the system of equations

$$\nabla L = 0 \quad \text{and} \quad \Phi_i = 0 \quad \text{for} \quad i = 1, ..., n \tag{1}$$

are called "pedal points", as these points of N cause local extrema of the distance function f to the given pentapod configuration ($M = \mathbb{R}^6$), position ($M = \mathbb{R}^3$) and orientation ($M = S^2$), respectively.

2 Linear in position variables

The design parameters of the linear pentapod used in the examples of Section 2 are:

$$\begin{array}{lllll} r_1 = 0 & r_2 = 1 & r_3 = 2 & r_4 = 4 & r_5 = 6 \\ x_1 = 0 & x_2 = -1/2 & x_3 = 1 & x_4 = -3 & x_5 = -1 \\ y_1 = 0 & y_2 = 0 & y_3 = 2 & y_4 = -1 & y_5 = 2 \end{array} \tag{2}$$

and $z_1 = \ldots = z_5 = 0$ due to the planarity of the base. This manipulator, which fits in with Theorem refthm:1, is in the given pose $\mathfrak{G} = (\frac{1}{3}, \frac{2}{3}, \frac{2}{3}, 1, 2, 3)$, which is non-singular.

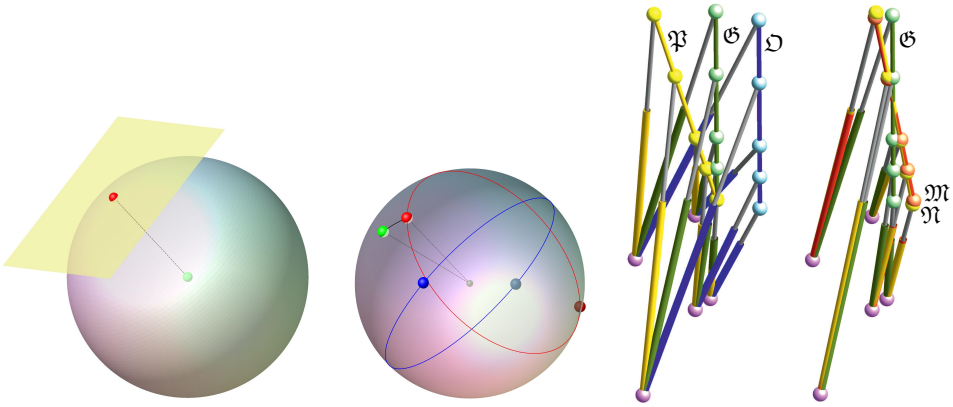

Fig. 2. Left: For fixed orientation the unique pedal point has coordinates $(\frac{61}{33}, \frac{38}{33}, \frac{92}{33}) \in \mathbb{R}^3$ which has a distance of 1.21854359 units from the given position. Middle-left: For fixed position the four pedal points are illustrated, where the one with coordinates $(0.12661404, 0.81506780, 0.56536126) \in \mathbb{R}^3$ is closest to the given orientation. The corresponding spherical distance equals 15.75049156°. The second pedal point is antipodal to the first one and the distance s is the supplementary angle. Illustration of the pose $\mathfrak{G}$ (green) of the linear pentapod studied in Section 2. Middle-right: The closest singular configurations in the position/orientation workspace are given by the pose $\mathfrak{P}$ (yellow) and $\mathfrak{O}$ (blue), respectively. Right: $\mathfrak{M}$ (red) is the closest singular pose under Euclidean motions of ℓ and $\mathfrak{N}$ (yellow) is the closest singularity under equiform motions of ℓ.

2.1 Fixed orientation case

We ask for the closest singular configuration $\mathfrak{O}$ having the same orientation (g_1, g_2, g_3) as the given pose $\mathfrak{G}$. The distance to the singularity pose with respect to (g_4, g_5, g_6) is computed according to the ordinary *Euclidean* metric. The singularity polynomial is linear in position variables and under fixed orientation condition it will be a plane *passing through the origin* in position space $\mathbb{R}^3$. Naturally, there will be only one pedal point and hence the number of solutions in this case will only be one.

Example 1. A general example with $\mathfrak{O} = (\frac{1}{3}, \frac{2}{3}, \frac{2}{3}, \frac{61}{33}, \frac{38}{33}, \frac{92}{33})$ is illustrated in Fig. 2.

2.2 Fixed position case

Now we ask for the closest singular configuration $\mathfrak{P}$, which has the same position (g_4, g_5, g_6) as the given pose $\mathfrak{G}$. In this case the distance to the singularity curve with respect to (g_1, g_2, g_3) is computed according to the *Riemannian distance s* on the sphere. This means that the shortest path between two poses on the sphere is the shorter curve of the *great circle* connecting the two points.

Under the fixed position the singularity polynomial factors into two planes in $\mathbb{R}^3$:

$$w(A_1u + A_2v + A_3w + A_4) = 0, \tag{3}$$

	u	v	w	s
1	0.12661404	0.81506780	0.56536126	15.75049156°
2	0.44721359	0.89442719	0	41.83152170°
3	-0.44721359	-0.89442719	0	138.25977700°
4	-0.60029825	-0.34138359	-0.72325600	155.56475890°

Table 1. The 4 real solutions in ascending order with respect to the spherical distance s to the given orientation.

where the design variables are encoded in the coefficients A_i.

As a consequence the *singular orientations* are obtained as the intersection of these two planes with the unit-sphere, which is given by the normalizing condition Γ. One of these planes always passes through the center of the sphere and hence the intersection is a great circle. For the second plane different cases can occur:

- $A_4^2 < A_1^2 + A_2^2 + A_3^2$: the plane intersects the sphere.
- $A_4^2 = A_1^2 + A_2^2 + A_3^2$: the plane is tangent to the sphere.
- $A_4^2 > A_1^2 + A_2^2 + A_3^2$: the plane doesn't intersect the sphere.

Depending on the case the total number of pedal points equals (a) 4, (b) 3 and (c) 2, respectively.

Remark 1. Note that if the given non-singular orientation is normal to one of the planes intersecting the unit-sphere, then there exists an infinite number of pedal points. ◇

Example 2. A general example with $\mathfrak{P} = (0.1266, 0.815, 0.5653, 1, 2, 3)$ is illustrated in Fig. 2. In the example at hand there exist 4 pedal points, which are listed in Table 1.

2.3 General case

Computing the distance to the next singularity for fixed orientation and position, respectively, are well-known concepts in kinematics but from these two separated informations no conclusion about the closeness to the next singular configuration within the 5-dimensional configuration space can be drawn. Therefore our general case deals with mixed (translational and rotational) DOFs, thus the question of a suitable distance function arises. As the configuration space $\mathscr{C}$ equals the space of oriented line-elements, we can adopt the object dependent metrics discussed in [9] as follows:

$$d(\mathfrak{L}, \mathfrak{L}')^2 := \frac{1}{5} \sum_{j=1}^{5} \|\mathbf{m}_j - \mathbf{m}_j'\|^2, \tag{4}$$

where $\mathfrak{L}$ and $\mathfrak{L}'$ are two configurations and $\mathbf{m}_j$ and $\mathbf{m}_j'$ denote the coordinate vectors of the corresponding platform anchor points. This metric has already been used in [6] for the mechanical device at hand. Note that this is an Euclidean metric in $\mathbb{R}^6$ comprised of the points (u, v, w, p_x, p_y, p_z).

	u	v	w	λ_1	λ_2	d
1	0.19954344	0.75426388	0.62551450	0.22471412	0.00242829	0.37163905
2	0.44721359	0.89442721	0.00000000	-1.18154819	0.15475648	1.53723662
3	-0.44720571	-0.89444123	0.00001503	-8.09845180	0.00888318	4.02454431
4	-0.72878205	-0.23306556	-0.64396839	-9.46430882	0.00812550	4.13597163
5	0.50116745	0.86532314	0.00686193	-1.24444052	63.53263267	4.98948239
6	-0.44100968	-0.89750916	-0.00554456	-8.10658006	-11.11676392	6.20308215

Table 2. The 6 real solutions in ascending order with respect to the distance d from $\mathfrak{G}$. The corresponding values of missing variables p_x, p_y, p_z are obtained by substituting $u, v, w, \lambda_1, \lambda_2$ into the expressions for p_x, p_y, p_z.

Remark 2. An alternative "closeness" index for linear pentapod with planar base can be based on a result of [10] that in singularity configurations legs with zero length can be constructed by the method of singularity-invariant leg-replacement. Therefore one can take the shortest length of the two-parametric set of length, which can be allocated, to evaluate the singularity "closeness". ◇

With respect to the metric d of Eq. (4), we can compute the closest singular configuration $\mathfrak{M}$ to $\mathfrak{G}$ in the following way: We determine the set of pedal-points on the singularity variety with respect to $\mathfrak{G}$ as the variety $V(\frac{\partial L}{\partial u}, \frac{\partial L}{\partial v}, \frac{\partial L}{\partial w}, \frac{\partial L}{\partial p_x}, \frac{\partial L}{\partial p_y}, \frac{\partial L}{\partial p_z}, \frac{\partial L}{\partial \lambda_1}, \frac{\partial L}{\partial \lambda_2})$ where λ_1 and λ_2 are the Lagrange multipliers of the Lagrange equation:

$$L(u, v, w, p_x, p_y, p_z, \lambda_1, \lambda_2) := d(\mathfrak{M}, \mathfrak{G})^2 + \lambda_1(u^2 + v^2 + w^2 - 1) + \lambda_2 F. \qquad (5)$$

Note that here F is the singularity polynomial linear in position variables (cf. [7]).

Example 3. Considering the example of the design parameters indicated in Eq. (2), there are 10 solutions out of which 6 are real[2]. These solutions were calculated as follows: After solving $\{\frac{\partial L}{\partial p_x}, \frac{\partial L}{\partial p_y}, \frac{\partial L}{\partial p_z}\}$ for $\{p_x, p_y, p_z\}$ and substituting the values obtained into the rest of the equations of the system, we can use the Gröbner basis method to solve the new system for the remaining variables. Using the order $w > v > u > \lambda_2 > \lambda_1$ one of the Gröbner basis generators solely depends on λ_1 while the rest depend on λ_1 and another orientation variable or λ_2, respectively. Based on this elimination technique Table 2 is obtained. The first row of this table corresponds to the global minimizer $\mathfrak{M}$ illustrated in Fig. 2, which has position variables $p_x = 1.42386285$, $p_y = 1.69623807$ and $p_z = 3.11364494$.

2.4 General case without normalizing condition

We can simplify the problem by considering equiform transformations of the linear platform ℓ, which is equivalent to the cancellation of the normalizing condition Γ. This would be equal to canceling the first constraint in Eq. (5). It turns out that for this reduced set of equations only 3 pedal points exit over $\mathbb{C}$.

[2] It is unknown if examples with 10 real solutions can exist.

	u	v	w	λ_1	λ_2	d
1	0.22077150	0.77922849	0.65664594	1.04265095	0.00209764	0.35854952
2	0.33333333	0.66666666	0	0.74535599	0.04901408	1.43604394
3	0.36256185	0.63743814	0.01002046	0.73340227	26.26334956	4.95602764

Table 3. The 3 real solutions in ascending order with respect to the distance d from $\mathfrak{G}$. The scaling factor of the corresponding equiform displacement of the platform is given by λ_1. The corresponding values of missing variables p_x, p_y, p_z are obtained by substituting u, v, w, λ_2 into the expressions for p_x, p_y, p_z.

Example 4. For the example under consideration, the computations can be done in the same way as in Section 2.3 with the sole difference that λ_1 is now absent. We end up with Table 3. The first row in this table corresponds to the global minimizer $\mathfrak{N}$ illustrated in Fig. 2, which has position variables $p_x = 1.36501824$, $p_y = 1.63498176$ and $p_z = 3.03249538$.

3 Linear in orientation variables

The design parameters of the linear pentapod used in the examples of Section 3 are:

$$\begin{aligned} &r_1 = 0 \quad r_2 = 1 \quad r_3 = 3 \quad r_4 = 5 \quad r_5 = 6 \\ &x_1 = 0 \quad x_2 = 1 \quad x_3 = -1/2 \quad x_4 = -3 \quad x_5 = -1 \\ &y_1 = 0 \quad y_2 = 0 \quad y_3 = 3/2 \quad y_4 = 4 \quad y_5 = 2 \end{aligned} \tag{6}$$

and $z_1 = \ldots = z_5 = 0$ due to the planarity of the base. It can easily be checked that this manipulator belongs to the first class of Theorem 2. Moreover we assume that this manipulator is in the given pose $\mathfrak{G} = (\frac{1}{3}, \frac{2}{3}, \frac{2}{3}, 1, 2, 3)$, which is non-singular.

3.1 Fixed orientation case

Once again we ask for the closest singular configuration $\mathfrak{O}$ having the same orientation (g_1, g_2, g_3) as the given pose $\mathfrak{G}$. The distance to the singularity pose with respect to (g_4, g_5, g_6) is computed according to the *ordinary Euclidean* metric. Under fixed orientation condition it is revealed that the singularity polynomial is factored to:

$$p_z(B_1 p_x + B_2 p_y + B_3 p_z + B_4) = 0, \tag{7}$$

where the design information is encoded in the coefficients B_i. For each of the two planes in $\mathbb{R}^3$ we can compute the pedal point with respect to the given pose (cf. Fig. 3).

Example 5. The closer pedal point implying $\mathfrak{O} = (\frac{1}{3}, \frac{2}{3}, \frac{2}{3}, 2, 3, 0)$ is displayed in Fig. 3.

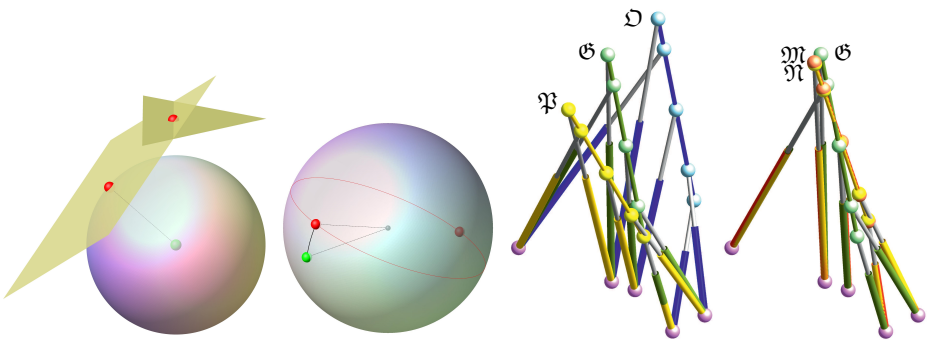

Fig. 3. Left: For fixed orientation there exits for each of the two planes a unique pedal point. One pedal point has coordinates $(-8/17, 9/17, 12/17)$ and a distance of 4.80196038 units to the given position and the other pedal point has coordinates $(2,3,0)$ and a distance of 4 units. Middle-left: For fixed position the two pedal points are illustrated, where the one with coordinate $(0.11346545, 0.47007115, 0.87530491)$ is closest to the given orientation. The corresponding spherical distance s equals 20.82450533°. Illustration of the pose $\mathfrak{G}$ (green) of the linear pentapod studied in Section 3. Middle-right: The closest singular configurations in the position/orientation workspace are given by the pose $\mathfrak{P}$ (yellow) and $\mathfrak{O}$ (blue), respectively. Right: $\mathfrak{M}$ (red) is the closest singular pose under Euclidean motions of ℓ and $\mathfrak{N}$ (yellow) is the closest singularity under equiform motions of ℓ.

3.2 Fixed position case

Now we ask again for the closest singular configuration $\mathfrak{P}$, which has the same position (g_4, g_5, g_6) as the given pose $\mathfrak{G}$. As the singularity polynomial is linear in orientation variables and does not possess an absolute term, the *singularity loci* is a *great circle* for the fixed position case. If the given orientation differs from the pole of the great circle, then there exist two pedal points (otherwise infinitely many).

Example 6. The results for the example at hand are displayed in Fig. 3, whereby the closer pedal point implies $\mathfrak{P} = (0.11346545, 0.47007115, 0.87530491, 1, 2, 3)$.

3.3 General Case

Similar "experimental" computations as in Section 2.3 show that there are again 10 solutions.

Example 7. For the example at hand we obtain 6 real solutions, which are given in Table 4. The first row in this table corresponds to the global minimizer $\mathfrak{M}$ illustrated in Fig. 3, which has position variables $p_x = 1.35978906$, $p_y = 2.34492506$ and $p_z = 2.57706069$.

3.4 General case without normalizing condition

Similar computations as in Section 2.4 show again that the number of solution reduces to three.

	u	v	w	λ_1	λ_2	d
1	0.24002202	0.57831003	0.77970951	-0.07616071	0.00198708	0.41484860
2	0.16067752	0.32134537	0.93924532	5.58789193	-0.03317073	2.44661840
3	-0.20843306	-0.55064498	-0.80863487	-10.27182281	0.00088059	4.53615852
4	-0.35275218	0.88481355	-0.34421986	-3.79940039	0.38394736	6.70384275
5	-0.02624291	-0.92437183	0.38072309	-7.13002767	0.19314992	7.16835476
6	-0.06268654	-0.12537309	-0.99012725	-32.85080126	0.07233642	9.04867032

Table 4. The 6 real solutions in ascending order with respect to the distance d from $\mathfrak{G}$.

	u	v	w	λ_1	λ_2	d
1	0.23632218	0.56965551	0.76841946	0.98530404	0.00196374	0.41349741
2	0.33333333	0.66666666	1.30046948	1.49892509	-0.02111913	1.81542685
3	-0.06965551	0.26367781	-0.10175277	0.29108677	3.26647730	6.49924087

Table 5. The 3 real solutions in ascending order with respect to the distance d from $\mathfrak{G}$.

Example 8. For the example at hand all three solutions are real and are given in Table 5. The first row in this table corresponds to the global minimizer $\mathfrak{N}$ illustrated in Fig. 3, which has position variables $p_x = 1.36986410$, $p_y = 2.36986410$ and $p_z = 2.61205791$.

Remark 3. Through the numerical examples one observes that the same number of pedal points is obtained for the other two geometries (items 2 and 3) listed in Theorem 2 for the computation of the closest singular pose under Euclidean motions of ℓ and equiform motions of ℓ, respectively. ◇

4 Conclusion

This article dealt with the computation of the singularity-free balls of two classes of simplified linear pentapods, namely, the linear pentapods with singularity polynomials linear position/orientation variables (abbreviated by LP/LO). It is demonstrated (cf. Section 2 and Section 3, respectively) that for these designs the computation simplifies considerably (cf. Table 6). One should note that the results obtained for singularity-free balls regarding manipulators with singularity varieties linear in position/orientation variables in the cases of *fixed position variables* and *fixed orientation variables* are general while for the *general case with normalizing condition* the given numbers are just based on a set of random examples[3]. Recently the authors were able to prove [8] that the pedal point problem in the *general case without normalizing condition* is a cubic one. Therefore the closest singular configurations under equiform motions (cf. Sections 2.4 and 3.4) are of interest, as they can be computed in closed form. This closed form solution offers interesting new concepts and strategies concerning real-time path planning/optimization; e.g. a variational path approach maximizing the distance to the singularity variety [8].

[3] In this context we also refer to Section 6 "What is a proof?" of [11], where the authors Faugere and Lazard were faced with a similar problem.

	Generic case	LP case	LO case
Fixed position	6	4	2
Fixed orientation	8	1	2
Object-oriented metric case	80	10	10
Object-oriented metric case without normalizing condition	28	3	3

Table 6. Illustration of the generic number of pedal points under different metric conditions. "Generic case" refers to the general pentapod (not necessarily with a simple singularity variety). Note that they are computed over the field of complex numbers and hence the real solutions might be lower. The red colored rows indicate that these numbers are just experimental while the green ones are mathematically proven and reliable in all situations.

Based on this closed form solution we also want to optimize the geometry of the pentapod such that for a given home-pose of the platform line the distance to the next singularity is maximal. This is dedicated to future research.

Acknowledgement The research is supported by Grant No. P 24927-N25 of the Austrian Science Fund FWF. Moreover the first author is funded by the Doctoral College "Computational Design" of Vienna University of Technology.

References

1. J. Borràs, F. Thomas, Singularity-invariant leg substitutions in pentapods, in: Intelligent Robots and Systems (IROS), 2010 IEEE/RSJ International Conference on, IEEE, 2010, pp. 2766–2771
2. M. Weck, D. Staimer, Parallel kinematic machine tools–current state and future potentials, CIRP Annals-Manufacturing Technology 51 (2) (2002) 671–683
3. C.-D. Zhang, S.-M. Song, Forward kinematics of a class of parallel (Stewart) platforms with closed-form solutions, Journal of Field Robotics 9 (1) (1992) 93–112
4. G. Nawratil, J. Schicho, Self-motions of pentapods with linear platform, Robotica (2015) 1–29
5. G. Nawratil, On the line-symmetry of self-motions of linear pentapods, in: Advances in Robot Kinematics 2016, Springer, 2018, pp. 149–159
6. A. Rasoulzadeh, G. Nawratil, Rational parametrization of linear pentapod's singularity variety and the distance to it, in: Computational Kinematics, Springer, 2018, pp. 516–524 (extended version on arXiv:1701.09107)
7. A. Rasoulzadeh, G. Nawratil, Linear pentapods with a simple singularity variety – part I: Determination and Redundant Designs, submitted to IFToMM World Congress 2019
8. A. Rasoulzadeh, G. Nawratil, Variational path optimization of pentapods with simple singularity variety, in preparation
9. G. Nawratil, Point-models for the set of oriented line-elements–a survey, Mechanism and Machine Theory 111 (2017) 118–134
10. J. Borras, F. Thomas, E. Ottaviano, M. Ceccarelli, A reconfigurable 5-dof 5-spu parallel platform, in: Proc. of ASME/IFToMM International Conference on Reconfigurable Mechanisms and Robots (ReMAR), IEEE, 2009, pp. 617–623
11. J.-C. Faugère, D. Lazard, Combinatorial classes of parallel manipulators, Mechanism and Machine Theory 30 (6) (1995) 765–776